Cell. Mol. Life Sci. (2015) 72:3999–4011
DOI 10.1007/s00018-015-1972-5

Cellular and Molecular Life Sciences

RESEARCH ARTICLE

Protease nexin-1 regulates retinal vascular development

Sonia Selbonne[1,2] · Deborah Francois[1,2] · William Raoul[3,4,5,6] · Yacine Boulaftali[1,2] · Florian Sennlaub[3,4,5] · Martine Jandrot-Perrus[1,2] · Marie-Christine Bouton[1,2] · Véronique Arocas[1,2]

Received: 17 February 2015 / Revised: 27 May 2015 / Accepted: 15 June 2015 / Published online: 25 June 2015

Abstract We recently identified protease nexin-1 (PN-1) or serpinE2, as a possibly underestimated player in maintaining angiogenic balance. Here, we used the well-characterized postnatal vascular development of newborn mouse retina to further investigate the role and the mechanism of action of PN-1 in physiological angiogenesis. The development of retinal vasculature was analysed by endothelial cell staining with isolectin B4. PN-1-deficient (PN-$1^{-/-}$) retina displayed increased vascularization in the postnatal period, with elevated capillary thickness and density, compared to their wild-type littermate (WT). Moreover, PN-$1^{-/-}$ retina presented more veins/arteries than WT retina. The kinetics of retinal vasculature development, retinal VEGF expression and overall retinal structure were similar in WT and PN-$1^{-/-}$ mice, but we observed a hyperproliferation of vascular cells in PN-$1^{-/-}$ retina. Expression of PN-1 was analysed by immunoblotting and X-Gal staining of retinas from mice expressing beta-galactosidase under a PN-1 promoter. PN-1 was highly expressed in the first week following birth and then progressively decreased to a low level in adult retina where it localized on the retinal arteries. PCR arrays performed on mouse retinal RNA identified two angiogenesis-related factors, midkine and Smad5, that were overexpressed in PN-$1^{-/-}$ newborn mice and this was confirmed by RT-PCR. Both the higher vascularization and the overexpression of midkine and Smad5 mRNA were also observed in gastrocnemius muscle of PN-$1^{-/-}$ mice, suggesting that PN-1 interferes with these pathways. Together, our results demonstrate that PN-1 strongly limits physiological angiogenesis and suggest that modulation of PN-1 expression could represent a new way to regulate angiogenesis.

Keywords Serpin · Angiogenesis · Retina · SerpinE2 · PN-1

Introduction

Angiogenesis is the growth of new blood vessels from existing ones and results from endothelial cell migration and proliferation. It is an essential process, not only for tissue/organ development but also for tissue remodelling following injury. Angiogenesis is tightly controlled by a physiological balance between stimulatory and inhibitory signals for blood vessel growth. In physiological conditions, the vascular network of adults is a stable system and angiogenesis occurs essentially during wound healing or in the uterus during the menstrual cycle. However, in pathological conditions such as ischaemic and inflammatory diseases or cancer, the angiogenic balance can be disturbed, leading to abnormal neovascularization. The switch

Electronic supplementary material The online version of this article (doi:10.1007/s00018-015-1972-5) contains supplementary material, which is available to authorized users.

✉ Véronique Arocas
veronique.arocas@inserm.fr

1 LVTS, INSERM, U1148, Paris, France

2 Univ Paris Diderot, Sorbonne Paris Cité, Paris, France

3 UMR_S 968, Institut de la Vision, Paris, France

4 Univ Paris 06, UPMC, Paris, France

5 Centre Hospitalier National d'Ophtalmologie des Quinze-Vingts, INSERM-DHOS CIC 503, 75012 Paris, France

6 Present Address: Université François-Rabelais de Tours, CNRS, GICC UMR 7292, Tours, France

to the angiogenic phenotype thus depends on a local change in the balance between pro- and anti-angiogenic molecules. Among the regulators of angiogenesis, members of the serpin superfamily such as antithrombin (AT) [1], pigment epithelium-derived factor (PEDF) [2] or PAI-1 [3] have been identified in different models in vitro and in vivo. Serpins form a large family of structurally related proteins present in the plasma or in tissues and play a central role in the regulation of protease activity. Many of them, including AT and PAI-1, are suicide inhibitors using a unique and extensive conformational change to inhibit proteases. However, some, like PEDF, are devoid of anti-protease activity [4] and both AT and PEDF play a role in angiogenesis independently of protease inhibition.

We recently identified protease nexin-1 (PN-1 or serpinE2), an inhibitory serpin, as a new player in the control of angiogenic balance [5]. PN-1 is the most efficient tissue inhibitor of thrombin, but also a powerful inhibitor of plasminogen activators [6, 7], proteases largely involved in tissue remodelling. It is expressed by nerve and vascular cells, essentially localized in the pericellular space. PN-1 is also secreted by platelets upon activation and is often found to be overexpressed at sites of tissue injury [8]. We have shown that PN-1 has an anti-angiogenic activity in vitro on HUVEC responses to VEGF, including proliferation, migration, capillary tube formation and on cell spreading on vitronectin. These effects were related to the interaction of PN-1 with endothelial cell glycosaminoglycans, but did not require the anti-protease activity of the serpin in vitro. Invalidation of the PN-1 gene in mice generates viable animals. PN-1-deficient mice (PN-$1^{-/-}$) do not present an obvious phenotype, with the exception of male infertility due to an altered semen protein composition [9]. However, in stress-related conditions, these mice develop abnormal responses indicating that PN-1 may be important for tissue repair. Indeed, they exhibit a significant delay in synapse reinnervation in a model of nerve regeneration [10] and an increased thrombosis response induced by vascular injury [11]. We have shown that the microvascular network sprouting from aortic rings derived from PN-$1^{-/-}$ mice was significantly enhanced compared to that of rings from wild-type (WT) mice [5].

In the present study, we further characterized the anti-angiogenic activity of PN-1, using the postnatal vascularization of the mouse retina as a model system to study physiological angiogenesis. The mouse retina is one of the best characterized models for in vivo vessel formation, as it occurs after birth and displays all of the processes involved in angiogenesis (i.e. sprouting, branching, fusion, remodelling and maturation) [12, 13]. Development of retinal blood vessels in mice occurs in the first week of postnatal life to form a highly organized two-dimensional vascular plexus. Blood vessels begin to form at the centre of the retina and the vascular plexus grows outwards towards the periphery to generate a regular alternating pattern of arteries and veins with an intervening capillary network. Our results show that PN-1 deficiency increased postnatal angiogenesis and resulted in hypervascularization of the retina. To our knowledge, such a phenotype with an increased number of veins and arteries has never been observed in genetically modified mice. Similar results were obtained in muscle and confirm that PN-1 is, as yet, an underestimated regulator of angiogenesis.

Materials and methods

Animals

Wild-type C57BL/6 and PN-1-deficient mice (PN-$1^{-/-}$) [14], backcrossed for 12 generations, were generated by heterozygous mating and bred in-house. The PN-1 genotype of animals was determined by PCR. All experiments were performed on littermates in accordance with French ethical laws and were approved by the local Ethics Committee (Comité d'éthique Paris Nord No. 121; 2011-14/69-0035).

PN-1/LacZ reporter mice were generated as previously described (PN-1 KI mice) [15]).

Whole-mount retina staining

At the designated postnatal time, the mouse eyes were enucleated and briefly fixed for 10 min in 4 % paraformaldehyde/PBS solution (PFA). Retinas were dissected and fixed in 4 % PFA at 4 °C overnight and washed before staining. Immunostaining was performed as described [16] using isolectin B4-Alexa 568 conjugate (Invitrogen), anti-NG2-Alexa 488 conjugate (Millipore), polyclonal anti-glial fibrillary acidic protein (GFAP) (Dako), monoclonal anti-α-smooth muscle actin-Cy3 conjugate (Sigma) or monoclonal anti-Ki-67-Alexa 488 conjugate (Cell signalling). An anti-rabbit IgG-Alexa 568 conjugate (Sigma) was used for GFAP staining. Retinas were flat mounted using Fluorescent mounting medium (Dako).

Retinal vessel growth was evaluated by measuring the ratio of the maximum length from the optic disc to the edge of the vessel to the retina length. The capillary density was estimated by the ratio of capillary area to the corresponding 100 × 300 μm area just behind the vascular front, using ImageJ software. Six to eight areas were analysed per retina. Other parameters: branch points, vessel thickness and length, number of segments and holes were measured by BioAnalyser software on at least four mice per group.

Isl+Ki67+ endothelial cells were manually scored in six random fields per retina of four mice per group.

Histology and frozen sections

Enucleated mouse eyes after removing of the lens and excised gastrocnemius muscle were embedded in optimal cutting temperature (OCT) compound in liquid nitrogen. Eyeballs were previously fixed for 10 min in 4 % PFA and incubated successively in 10, 20 and 30 % sucrose solutions for 2 h each. Sections (10 μm) were cut in a cryostat, placed on glass slides and allowed to dry for 20 min.

For histology, eyes were fixed in 0.5 % glutaraldehyde, 4 % PFA for 2 h, dehydrated and mounted in historesin. 5 μm sections were cut and stained with toluidine blue.

X-Gal staining

Whole retinas were fixed for 15 min in 4 % PFA and retinal sections for 5 min in 0.5 % glutaraldehyde and then incubated at 37 °C with X-Gal staining solution (20 mM potassium ferricyanide, 20 mM potassium ferrocyanide, 5 mM $MgCl_2$, 1 mg/ml X-Gal in PBS).

Protein analysis

Eyes from pups or adult mice were removed and briefly fixed for 10 min in 4 % PFA. The retinas were dissected out, washed and lysed (two retinas per lysate) in 0.1 ml of RIPA buffer (50 mM Tris, pH 7.4, 150 mM NaCl, 1 % NP40, 1 % sodium deoxycholate, 0.1 % sodium dodecyl sulphate) containing a cocktail of protease inhibitors (1:100; Sigma), briefly sonicated and centrifuged at 10,000*g* at 4 °C. The supernatant was recovered and the protein concentration was determined using the BCA protein assay (Pierce).

Immunoblotting

Samples (30 μg) were electrophoresed in 4–20 % polyacrylamide gel (Pierce) and electrotransferred to nitrocellulose or PVDF membrane.

Immunoblotting was performed with anti-PN-1 monoclonal 4B3 (Santa Cruz), monoclonal rabbit anti-Smad5 (Cell Signalling), polyclonal anti-midkine (Santa cruz) or monoclonal anti-β actin (Abcam), followed by goat anti-rabbit or anti-mouse secondary antibodies-HRP conjugate (Jackson).

VEGF

VEGF was quantified in retinal lysates using mouse VEGF ELISA (Quantikine, R&D).

Antibody array

Analysis of the expression profile of angiogenesis-related proteins was performed on WT and PN-$1^{-/-}$ retina lysates at postnatal days 2 using an angiogenesis antibody array (Proteome Profiler Mouse Angiogenesis Array kit, R&D). Lysates of four retinas in 0.1 ml of buffer [1 % Triton X 100 in PBS, containing a cocktail of protease inhibitors (Sigma)] were used. Positive signals were quantified using Bio1D software.

RNA analysis

Quantitative reverse transcription real-time PCR (qRT-PCR)

Total RNA was extracted from pools of 16 retinas at P2 or extracted from the tibialis muscle after crushing, using TRIzol Reagent (Invitrogen) according to the manufacturer's protocol.

RNA was reverse-transcribed into cDNA using oligo dT primers and Superscript II Reverse Transcriptase (Invitrogen). Real-time PCR was performed on cDNA with Light Cycler FastStart DNA Master plus SYBR Green I (Roche Applied Science) and using the primers listed in supplementary material (Table SI). The level of expression of the target gene was normalized to that of Hsp90ab1 for retina or that of GAPDH for the tibialis muscle in each sample.

Microarray

The expression profile of 84 key angiogenesis-related genes was analysed using the RT^2 Profiler Angiogenesis PCR array according to the manufacturer's protocol (Qiagen). Total retinal RNA was extracted from pools of ten retinas at P2 using TRIzol Reagent (Invitrogen). RNA was purified using RNase-free Dnase I and RNeasy MinElute Cleanup kit, according to the manufacturer's instructions (Qiagen). First-strand cDNAs were synthesized from 1 μg of total RNA using the RT^2 First Strand Kit. Amplification and detection was then performed with RT^2SYBR Green Mastermix in CFX96 Real time System C1000 Thermal Cycle (Bio Rad). The average ΔC_t value for each gene and each treatment group across triplicate arrays was calculated and normalized using Hsp90ab1. $\Delta\Delta C_t$ for each gene were determined for WT and PN-$1^{-/-}$ samples and the fold change was calculated using the formula: fold change $= 2^{(-\Delta\Delta C_t)}$.

Results

PN-1-deficient retinas have an increased vasculature

In the newborn mouse retina, an organized two-dimensional vascular architecture develops from the optic disc to

the periphery of the retina during the early postnatal period. By staining endothelial cells with isolectin B4, we compared the retinal vascular development in WT and PN-1-deficient littermates on flat-mount retinas (Fig. 1). PN-1 deficiency did not modify the radial vascular expansion and kinetics of vessel development. Indeed, the growth of the vascular plexus between the optic disc and the periphery during the first postnatal week was similar for the WT and PN-$1^{-/-}$ retinas (Fig. 1a, arrows and quantification). However, analysis of the retinal vascular network demonstrated a very significant enhancement of postnatal angiogenesis in the retina of PN-$1^{-/-}$ mice compared to WT mice. Indeed, we observed an increase in the capillary density in PN-$1^{-/-}$ retinas (Fig. 1b), as confirmed by densitometric analysis that revealed a significant increase from postnatal day 4 (P4) to P7 (Fig. 1b). Moreover, the number of branch points, capillary thickness and length, and the number of intercapillary spaces were all significantly increased in PN-$1^{-/-}$ retina (Fig. 2).

Arteries and veins can easily be distinguished by morphological criteria. Retinal arteries are indeed surrounded by capillary-free zones, whereas veins, which alternate with arteries, are not, and tend to be slightly wider than arteries [17]. Remarkably, we observed that the number of veins/arteries was higher in PN-$1^{-/-}$ than in WT mice retinas (Fig. 3). Indeed, we observed five veins and five arteries in most WT retinas, whereas this number was increased in most PN-$1^{-/-}$ retinas, with six or seven veins and arteries (Fig. 3d). This difference was observed as soon as veins and arteries could be distinguished, i.e. around P4, and was still apparent in adult retinas (Fig. 3c).

These results thus indicate an obvious difference in the characteristics of the vasculature of PN-1-deficient retina, with an increased capillary density and also an increased number of major vessels, compared to WT.

PN-1 is highly expressed at the early stages of retinal vascular development

PN-1 expression was analysed by western blotting of WT retinal lysates at different postnatal times with a monoclonal anti-PN-1 antibody. As previously observed in different cell lines and tissues [18–21], PN-1 was detected as a 50 kDa migrating protein (Fig. 4a). Following birth, PN-1 protein expression was high, increased transiently with a maximum around postnatal day 3 (P3) and then progressively decreased to an almost undetectable signal in adult retina (Fig. 4a). The pattern of PN-1 expression was

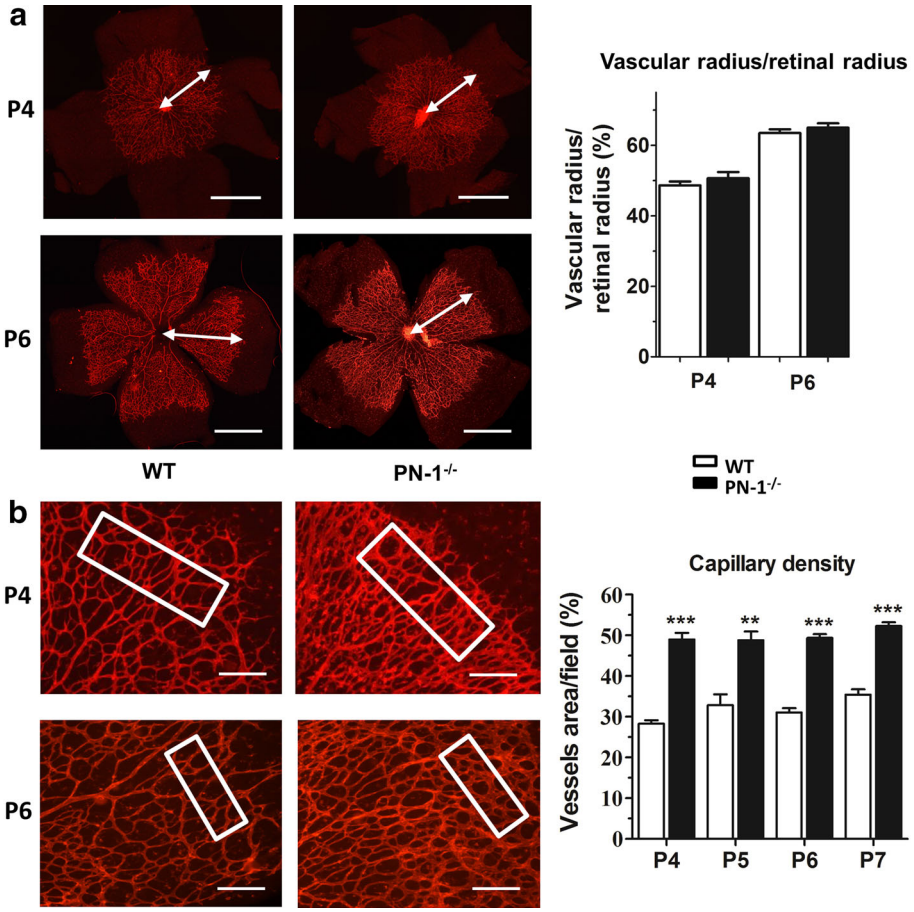

Fig. 1 Vascularization of the retina of 4- and 6-day-old pups (P4 and P6, respectively) was analysed by endothelial cell staining with isolectin B4 (in *red*). Flat-mount retina from wild-type (WT) and PN-1-deficient mice (PN-$1^{-/-}$) are shown. **a** Total retina, *scale bar* 1 mm. The vascular radius indicated by *arrows* was measured, and the results were expressed as the percentage of retinal radius (3–4 sections per retina, $n \geq 4$ retinas from different animals). **b** Magnification, *scale bar* 150 µm at P4, 100 µm at P6. Representative images are shown. Capillary density was analysed after magnification of the 100 × 300 µm areas indicated by *rectangles* and quantified as the percentage of area covered by vessels (6–8 sections per retina, $n \geq 4$ retinas from different animals)

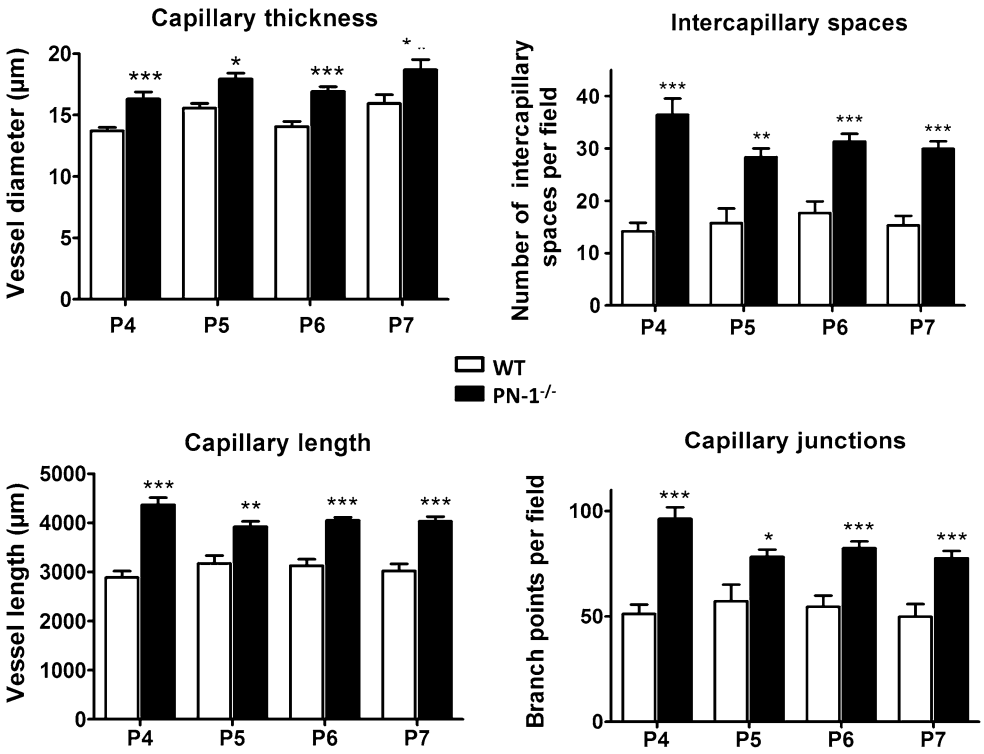

Fig. 2 PN-1 deficiency is associated with an increased retinal vascularization. Quantification of capillary thickness, length, number of junctions and of intercapillary spaces was performed on the areas indicated in Fig. 1b using the Biologic Analyser Software (6–8 sections per retina, $n \geq 4$ retinas from different animals). $^{*}p < 0.05$, $^{**}p < 0.01$, $^{***}p < 0.0001$ vs. WT

also analysed by X-Gal staining of PN-1/LacZ retina, in which β-galactosidase activity reported PN-1 expression (Fig. 4b-d and increased magnification in supplemental Fig. S2). The expression of PN-1 was intense and wide in the retina with a peak at P3 (Fig. 4b). Later, it increased progressively in the retinal vessels, but decreased in other areas. Both our immunoblotting results and X-Gal staining of PN-1/LacZ retina thus indicate a wave of PN-1 during retinal vascular development. The localization of PN-1 was then mostly restricted to the retinal arteries (distinguished from veins by their distinct morphologies), where it was essentially detectable in the adult (Fig. 4b, c).

In addition to the retinal vascular development, the neural retina undergoes considerable remodelling during this developmental program, with the formation of the inner and outer nuclear layers (INL and ONL, respectively, supplemental Fig. S1). X-Gal staining of PN-1/lacZ retinal sections indicated that the cells expressing PN-1 were localized in all developing retinal cell layers as well as in the choroid (Fig. 4d) up to P8, and then progressively localized to the ganglion cell layer (GCL) and to the inner and outer edges of the inner nuclear layer (INL). From P8, PN-1 expression was observed only in these vascularised layers (Fig. 4d).

PN-1 deficiency does not alter retinal structure

To analyse whether the difference in retinal vasculature could be related to structural retinal differences in WT and PN-$1^{-/-}$ mice, we compared retinal sections histologically. PN-$1^{-/-}$ retinas presented a normal retinal cell organization in three layers of nerve cell bodies (GCL, INL and ONL) and two layers of synapses, similar to WT retinas (Fig. 5a). As astrocytes and pericytes are determinants of vascular guidance and maturation, respectively, we also examined their retinal distribution by immunostaining of either PDGFRα, GFAP or NG2 on whole-mount retinas. Pericyte coverage (NG2 labelling) of the vessels (isolectin labelling) (Fig. 5b) as well as distribution and maturation of retinal astrocytes across the retina (PDGFRα and GFAP labelling Fig. 5c) was similar in PN-$1^{-/-}$ retinas compared with WT. Together, these observations indicate that the higher retinal vascular network in PN-$1^{-/-}$ mice is not due to a modification of the overall retinal structure or of a scaffold effect of astrocytes.

Endothelial cell proliferation is increased in PN-1-deficient retina

Isolectin B4 labelling of the angiogenic front revealed that the number and morphology of endothelial tip cells and filopodia were similar in WT and PN-$1^{-/-}$ retinas (Fig. 6a). However, quantification of proliferating endothelial cells (Isl+Ki67+ cells) indicated that proliferation was higher in PN-$1^{-/-}$ than in WT retinas at the vascular front (Fig. 6b), in agreement with our previous in vitro data [5].

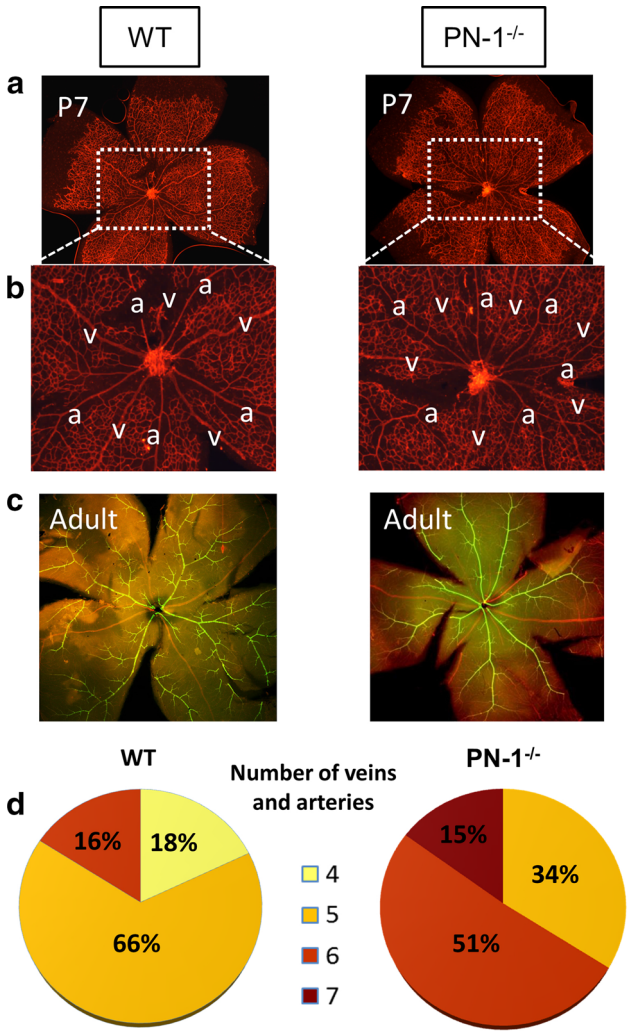

Fig. 3 PN-1 deficiency is associated with an increased retinal vascularization—quantification of retinal veins and arteries. **a** Whole-mount WT and PN-$1^{-/-}$ P7 retinas were stained with isolectin B4; *rectangles* bordering the central optic nerve area are shown in higher magnification in **b**. **c** Vascularization of adult retina. Flat-mount retinas were immunostained with antibody to smooth muscle alpha actin (in *green*) to reveal mainly retinal arteries. Representative images from at least three different animals are shown. **d** The number of retinal veins and arteries was counted manually. It ranged from 4 to 7 in WT and PN-$1^{-/-}$ retina (mice from P4 to adult age were pooled, with $n = 40$ for each genotype). For each genotype, the number of retinas having four, five, six or seven veins and arteries was compiled, and the results were expressed as the percentage of the total number of retinas

PN-1 deficiency results in an increase of midkine and Smad5 expression

As endothelial cells respond to VEGF gradients by tip cell formation and guide migration in the developing mouse retina, [16], we compared VEGF levels in retinal lysates from WT and PN-$1^{-/-}$ mice by ELISA. Results revealed similar expression for VEGF during postnatal development in WT and PN-$1^{-/-}$ retinas from P1 to P10 (Fig. 7a). In both types of mice, VEGF levels increased from P1 to P3 and then decreased to P6, before increasing again to P8 and going back to significantly lower levels from P10 to adult, in agreement with the kinetic of expression of VEGF mRNA previously observed in WT retinas and according to the two phases of vascular development [22].

To better understand how PN-1 regulates retinal vascular development, we performed comparative antibody and PCR arrays on retinal lysates and RNA, respectively, from P2 PN-$1^{-/-}$ and WT mice. The relative expression levels of 53 mouse angiogenesis-related proteins was analysed and compared using the mouse angiogenesis proteome profiler array, including growth and differentiation factors, extracellular matrix components, proteases, membrane-bound receptors and intracellular signalling molecules. However, no significant difference in protein expression between PN-$1^{-/-}$ and WT mice was observed for any of the factors analysed ($n \geq 3$ lysates per mouse type) (supplemental Table II). The expression of other angiogenic factors was assessed using the Mouse Angiogenesis RT^2 Profiler PCR Array, and a few of them, corresponding to major angiogenic proteins, were also analysed in the antibody array (supplemental Table III). Of the 84 genes analysed, only 2 appeared to be significantly differentially expressed in WT and PN-$1^{-/-}$ mice, the neurite growth factor 2 midkine (MK) (1.98 fold, $p = 0.04$) and the signal mediator for bone morphogenic protein (BMP) Smad5 (1.39 fold, $p = 0.002$). Increased mRNA expression in PN-$1^{-/-}$ was confirmed for both factors by conventional RT-PCR (1.6-fold for midkine, $p = 0.0218$, and 2.8-fold for Smad5, $p = 0.0001$) (Fig. 7b). PCR array analysis indicated also a tendency for increased expression of transforming growth factor beta receptor I (TGFβR1) and hypoxia-inducible factor 1 alpha subunit (Hif1α) in PN-$1^{-/-}$ compared to WT mice. However, TGFβR1 and Hif1α expressions were comparable in PN-$1^{-/-}$ and WT retinas when analysed by conventional RT-PCR.

Protein analysis of MK and Smad5 was performed by immunoblotting of retinal lysates from WT and PN-$1^{-/-}$ pups (Fig. 7c). MK was detected at ~16 kDa in both WT and PN-$1^{-/-}$ at P4. Densitometric analysis of the blots indicated a significantly increased expression of MK in PN-$1^{-/-}$ retinas. In contrast, the expression of Smad5 protein, detected at ~60 kDa, was similar in WT and PN-$1^{-/-}$ retinas (Fig. 7c).

PN-1-deficient mice have also more vessels in the muscle

We also analysed the effect of PN-1 deficiency in another mouse tissue to determine if our observations were specific

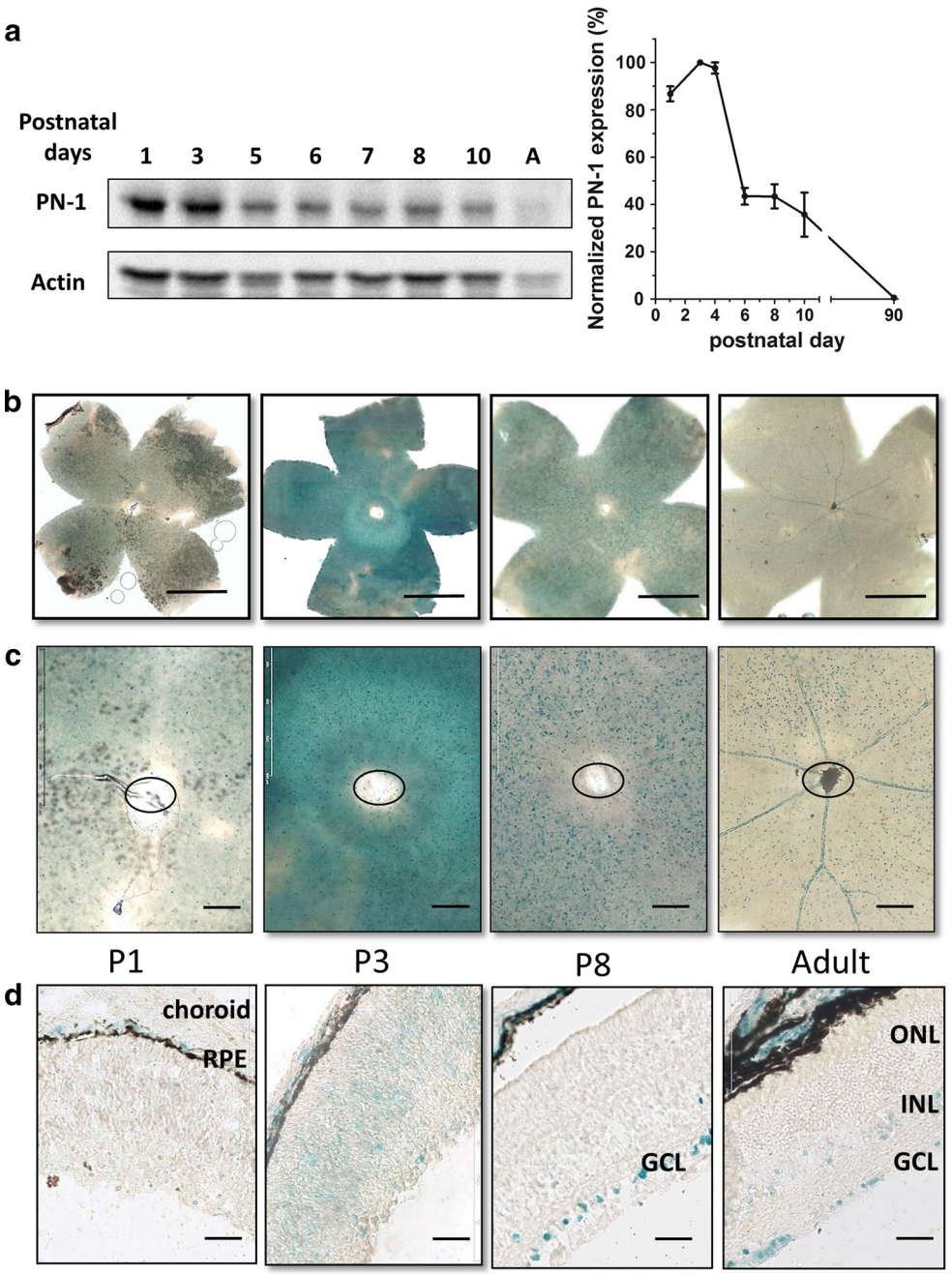

Fig. 4 PN-1 expression in mouse retina. **a** PN-1 expression in retinal lysates was analysed by immunoblotting at different postnatal ages, and results were quantified by densitometric analysis. A representative blot out of three blots performed on three different sets of retina is shown on the *left*, and on the *right*; the corresponding results (analysis of 6 retinas per age) are expressed as the percentage of the maximal expression, observed at P3. X-gal staining of whole-mount PN-1/LacZ retina. **b** Whole retina. **c** Magnification of the optic nerve area of the image shown in **b**. *Circles* represent the optic nerve head region. No staining was observed in retinas from WT mice. **d** X-gal staining of PN-1/LacZ retinal cross sections. *INL* inner nuclear layer, *GCL* ganglion cell layer, *RPE* retinal pigment epithelium. Representative images are shown out of at least three different animals. *Scale bars* 1 mm in **b**, 200 μm in **c**, 50 μm in **d**

or not to the retina. Because adult skeletal muscle is highly vascularized to support oxygenation and metabolic demands of this tissue, we analysed vascularization of the gastrocnemius muscle. Isolectin (Fig. 8a) and smooth muscle actin (Fig. 8b) labelling of endothelial cells and smooth muscle cells, respectively, in gastrocnemius muscle also indicated a significantly increased vascularization in PN-$1^{-/-}$ muscle compared with WT muscle. RT-PCR on muscle mRNA also evidenced increased expression of midkine and Smad5 in this tissue (Fig. 8c), confirming the effect of PN-1 deficiency on the expression of these genes, independently of the tissue.

Discussion

In the murine eye, intra-retinal vessels begin to spread outward from the optic disc towards the retinal periphery after birth. Large vessels extend towards the retinal periphery and capillaries infiltrate the areas between them.

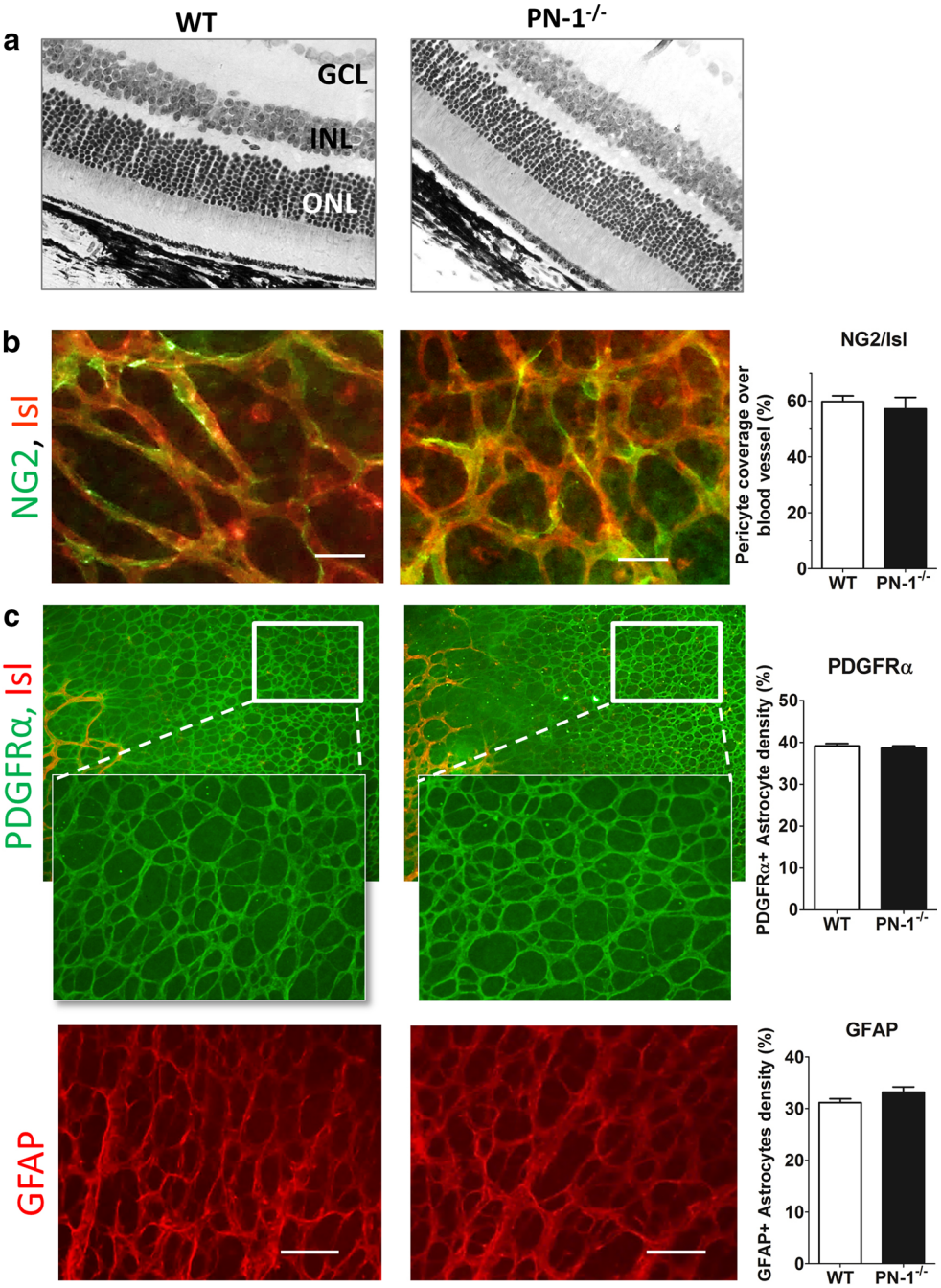

Fig. 5 Retinal structure, pericyte coverage and astrocyte template are not modified by PN-1 deficiency. **a** Histological sections of historesin-embedded eyes from adult WT and PN-$1^{-/-}$ mice. *GCL* ganglion cells layer, *INL* inner cells layer, *ONL* outer cell layer. **b** In *green*, pericyte coverage was visualized by NG2 immunostaining of P4 retinas, together with endothelial cells staining by isolectin in *red*. *Scale bars* 30 µm. **c** Astrocyte distribution was visualized by PDGFRα and GFAP immunostaining of P4 retinas, *scale bars* 50 µm. PDGFRα and GFAP positive astrocytes were analysed in avascular and vascularized areas, respectively. Representative images are shown. Quantifications indicate no difference in any of the markers analysed between WT and PN-$1^{-/-}$ retinas (4–6 fields par retina from at least 3 different animals)

Our results show an original phenotype that has, to our knowledge, never been described before in gene-deficient mice. Indeed, PN-1 deficiency appears to be associated with hypervascularization, characterized not only by an increased retinal capillary density in the first 7 days following birth, but also by an increased number of veins and arteries that persisted in adult mice.

In addition to endothelial cells, other cells including smooth muscle cells, pericytes, fibroblasts and glial cells have been shown to express PN-1 [19, 23–27]. Therefore, several retinal cell types could be a source of PN-1 in the retina. Accordingly, we observed that PN-1 is ubiquitously expressed in the retina in the first few days following birth. This expression increases after birth and then decreases to reach a low level in adults, in agreement with a potential role in vessel development. Indeed, Dorell et al. have shown a correlation between the expression profile of different retinal genes and the specific postnatal developmental events in which they are involved [28]. The expression profile of PN-1 that we describe is similar to the

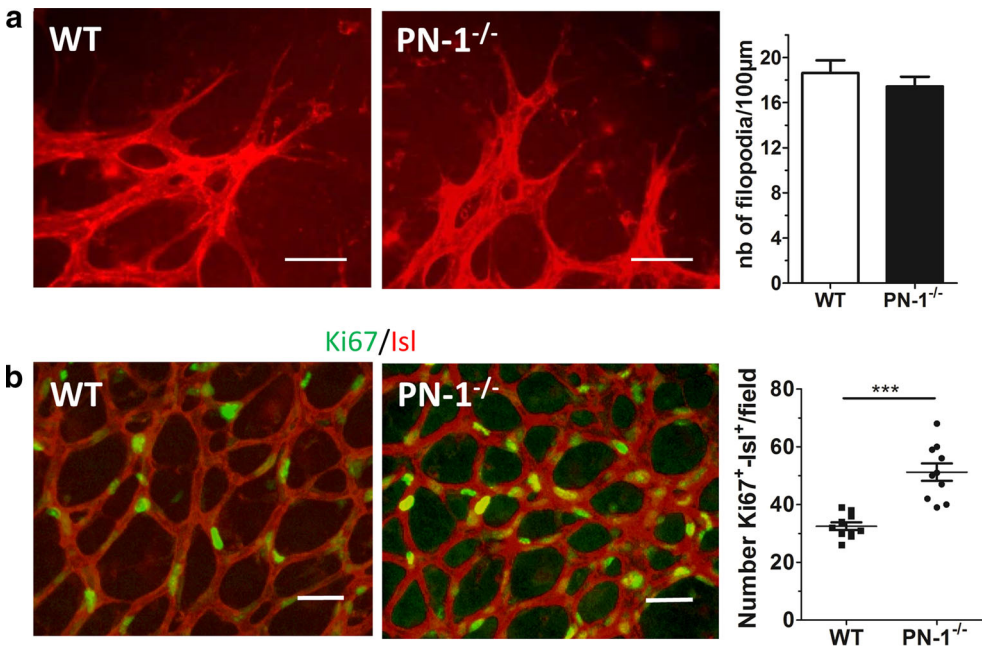

Fig. 6 PN-1 deficiency does not modify retinal tip cells, but increases endothelial cell proliferation. **a** Vessels were visualized by isolectin B4 staining of P5 WT and PN-$1^{-/-}$ retinas. Images of angiogenic front and quantification of filopodia in WT and KO retinas reveal no difference in tip cells. Representative images are shown (4 fields par retina, ≥3 different animals), *scale bar* 30 µm. **b** P5 retinas were stained with isolectin B4 (Isl, *red*) and an antibody against KI67 (*green*). *Scale bar* 50 µm. Representative images (4 fields per retina, 4 retinas from different animal of each genotype) and quantification of proliferating (Ki67+) endothelial cells (Isl+) are shown

profile of other genes, described by Dorell et al., having the highest expression during retinal vascularization, such as angiopoietin-2 and platelet-derived growth factor-receptor (PDGFαR). The very strong PN-1 expression in the early postnatal days of developing vasculature could thus be a way of controlling angiogenesis and allowing for a proper initiation of vascular development in the retina. This expression then rapidly decreases, but would still be sufficient to control angiogenesis throughout the process of vasculature development. In adult mice, while minimal PN-1 expression persists all over the retina, the main expression site is in the arteries, in agreement with previous data showing the expression of PN-1 in arterial smooth muscle cells and endothelial cells [24]. This persistent vascular expression is assumed to have a protective effect, according to the previous results on PN-1 functions in blood vessels [8].

Interactions between endothelial cells, astrocytes and neuronal cells are crucial for fine capillary network formation by endothelial cells. Astrocytes have a crucial role in guiding endothelial tip cells in the vascular branch and in the proliferation of endothelial stalk cells behind the tip cells [29, 30]. We thus examined astrocyte distribution and maturation in the retina of PN-$1^{-/-}$ mice compared to WT mice. We observed a similar astrocyte template and no difference in tip cells in PN-$1^{-/-}$ and WT retina. Therefore, although PN-1 was originally defined as a protein expressed by glial cells and named the glia-derived nexin [31], PN-1-deficient astrocytes appear to have a normal angiogenic function in the retina. Pericytes are also important players in vascular development. They are known to function by stabilizing blood vessels and have recently been shown to promote selective vessel regression [32]. We observed a normal arteriovenous pattern with no malformations and normal pericyte recruitment in PN-$1^{-/-}$ retinas, despite the higher number of veins and arteries compared with WT retinas. However, the increased vascular density was associated with greater endothelial cell proliferation, in agreement with our previously described in vitro studies [5]. The absence of PN-1 thus appears to primarily affect early processes, i.e. reorganization and proliferation of endothelial cells rather than vessel maturation or stabilization processes.

Other serpins involving or not serine protease inhibition are known to regulate angiogenesis in the retina. The inhibitor PAI-1 was shown to exert both pro-and anti-angiogenic activities via effects on extracellular matrix proteolysis and cell adhesion [3, 33]. Interestingly, in contrast to PN-1 deficiency, PAI-1 deficiency was associated with decreased angiogenic responses in the retina in a model of oxygen-induced retinopathy [34]. The non-inhibitory serpin PEDF has also been reported to be an important anti-angiogenic factor in the retina. PEDF deficiency was associated with a significantly faster spreading

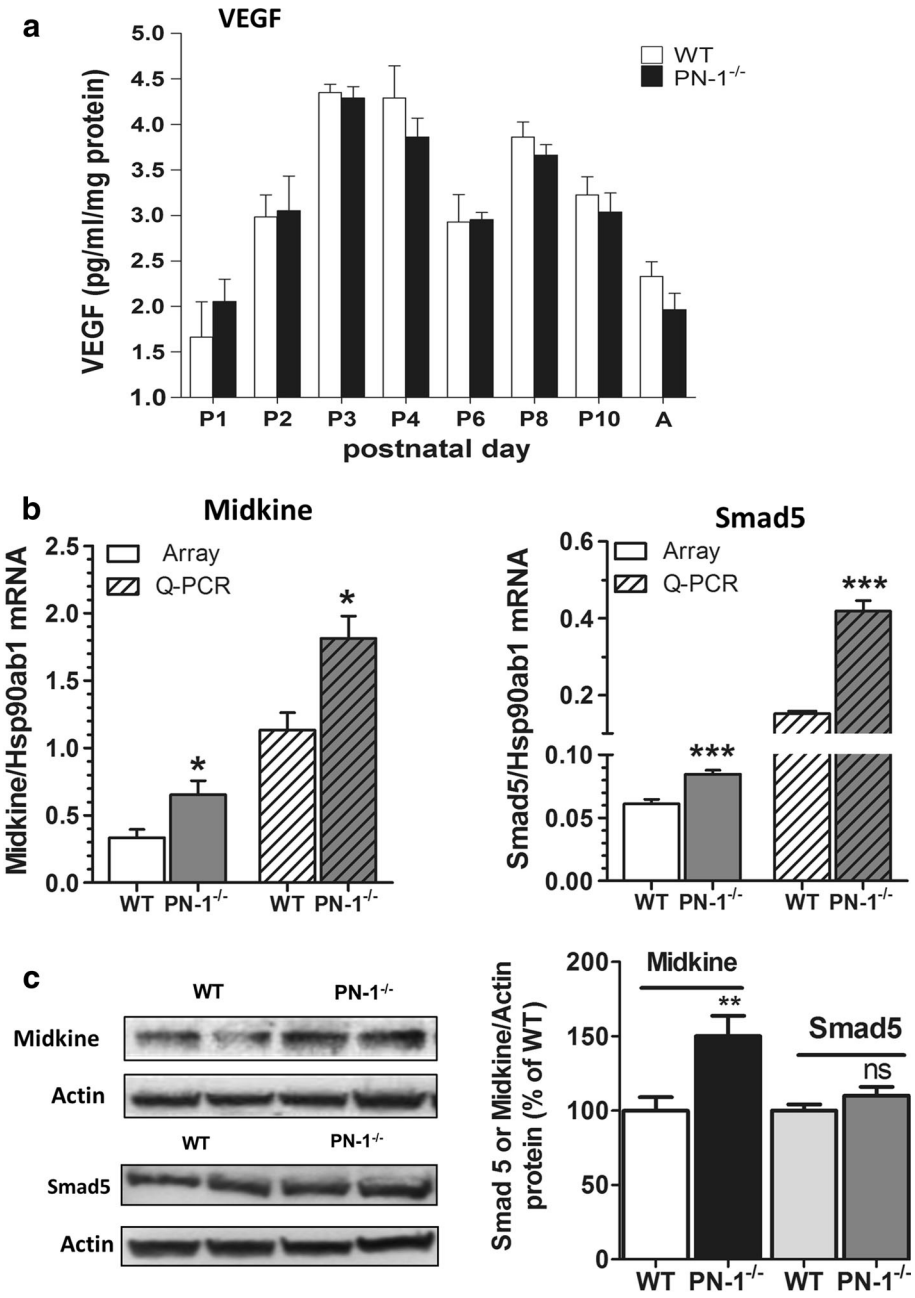

Fig. 7 PN-1 deficiency does not modify VEGF level, but increases midkine and Smad5 expression in the retina. **a** VEGF was quantified by ELISA in retinal lysates ($n = 3$–5 from different animals). **b** Gene expression analysis by PCR-based micro array and conventional RT-PCR on retinal mRNA revealed increased expression of midkine and Smad 5 ($n \geq 3$ experiments). **c** Representative immunoblots of P4 retinal whole lysates with antibodies to midkine or Smad5 ($n \geq 3$ immunoblots performed on different sets of retina) and densitometric analysis of the blots, expressed as mean intensity (midkine or Smad5/actin ratio) relative to WT, determined for each immunoblot. $^{*}p < 0.05$, $^{**}p < 0.001$, $^{***}p < 0.0001$ vs. WT, *ns* non-significant

of retinal vessels without any difference in vessel number compared to WT mice [35]. Thus apart from their roles as protease inhibitors, serpins are also important players in the retinal angiogenic balance and may contribute to the regulation of angiogenesis. Although we have previously shown that a recombinant variant of PN-1 devoid of anti-protease activity retained its anti-angiogenic activity [5], a contribution of PN-1 anti-protease activity in vivo cannot be ruled out. PN-1 may regulate angiogenesis by several mechanisms due to its interactions with many partners involved in angiogenesis, including proteases (thrombin and plasmin in particular) or GAGs and matrix proteins (vitronectin). Through its anti-protease activity, PN-1 could reduce cell surface receptor shedding, cleavage of adhesive proteins and matrix degradation by proteases. In addition, PN-1 may modulate the interaction of cytokines and matrix proteins with their membrane receptors, independently of its anti-protease activity by competitive binding.

To further understand the anti-angiogenic activity of PN-1, VEGF levels and antibody and PCR arrays dedicated to angiogenesis were performed, respectively, on retinal protein and RNA lysates. The expression of VEGF was not modified by PN-1 deficiency. Antibody array evidenced no

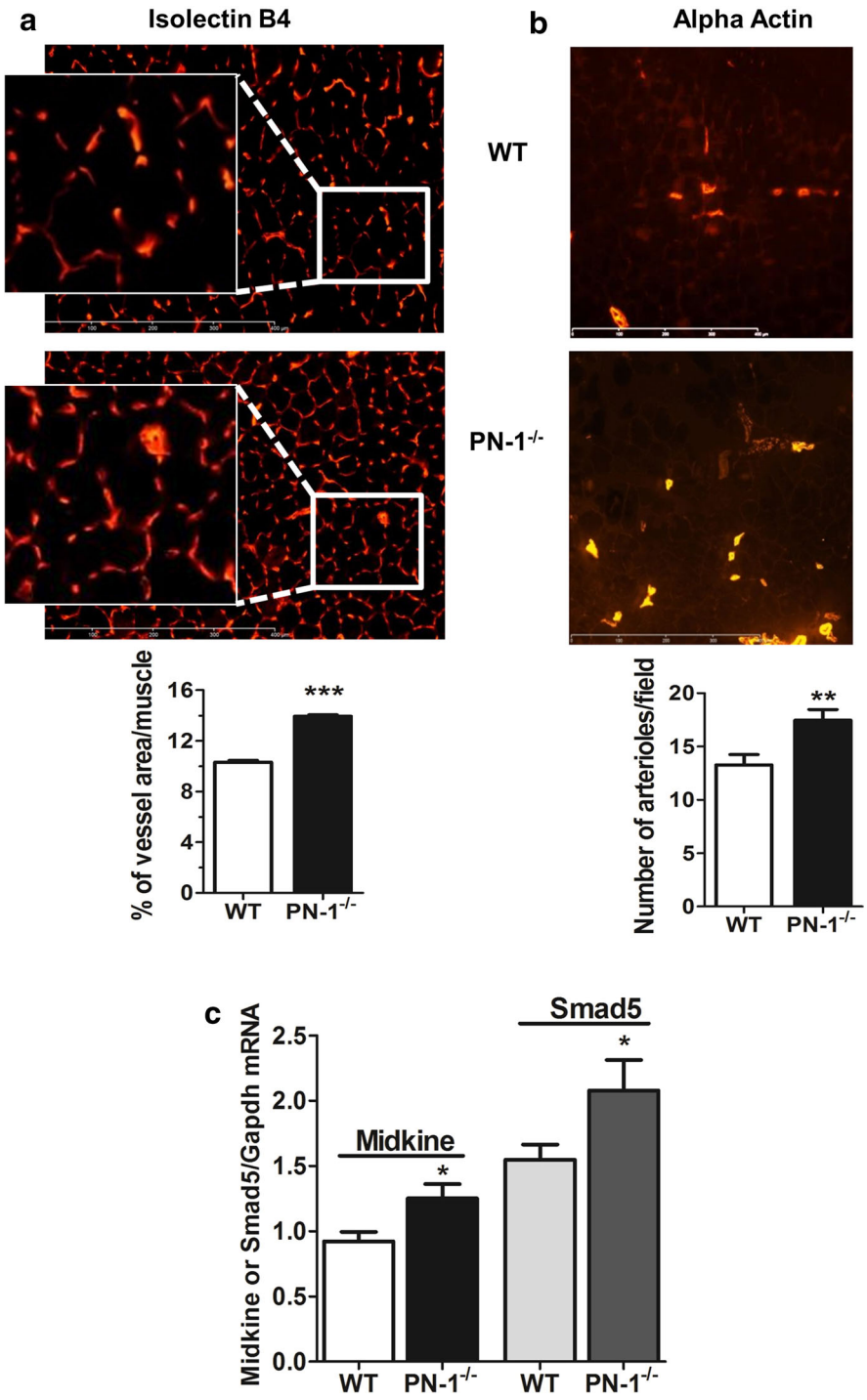

Fig. 8 In gastrocnemius muscle, PN-1 deficiency is also associated with increased vascularization and increased expression of midkine and Smad5. Muscle sections were stained with isolectin B4 (**a**) or with smooth muscle alpha actin (SMA) (**b**). Representative images are shown from at least four different animals. Vascular coverage was quantified by densitometric analysis of isolectin images and arterioles were counted manually on SMA images. $^{**}p < 0.01$, $^{***}p < 0.001$ vs. WT. **c** Midkine and Smad5 mRNA levels were compared in WT and PN-$1^{-/-}$ tibialis muscles by RT-PCR ($n = 26$)

significant difference in the expression of any of the 53 angiogenesis-related factors analysed, between WT and PN-$1^{-/-}$ retinas. However, a PCR array allowing the analysis of genes that were not tested in the antibody array identified significantly increased expression of two genes in PN-$1^{-/-}$ retina, midkine (MK) and Smad5. MK is a heparin-binding growth factor that has been shown to promote angiogenesis both in tumours [36] and in response to ischaemia [37]. Smad5 is a transcription factor involved in the TGF-beta signalling pathway. Smad5-deficient embryos have enlarged blood vessels characterized by decreased content in vascular smooth muscle cells, massive apoptosis of mesenchymal cells and endothelial cells that do not display angiogenic responses in vitro [38]. Conversely, in PN-1-deficient mice, Smad5 overexpression could result in the modulation of the Smad5 signalling

pathway and, together with MK-induced proangiogenic effects, contribute to the increased vascular development associated with PN-1 deficiency. However, overexpression of Smad5 gene did not correlate with Smad5 protein level, minimizing its potential role in the vascular phenotype of PN-1-deficient mice. In contrast, overexpression of MK was confirmed at the protein level in PN-1-deficient mice and could thus be of importance for the PN-1 phenotype.

In support of our major finding in the retina, we obtained similar results in another highly vascularized mouse tissue, the hindlimb calf muscle. Indeed, we observed an increased capillary density, together with an increased number of arterioles, in the gastrocnemius of PN-$1^{-/-}$ mice, compared with that of their control littermates. In addition, we also found a higher expression level of MK and of Smad5 in PN-$1^{-/-}$ calf muscle than in WT muscle. PN-1 deficiency thus appears to induce a general phenotype of high vascularization, although this phenotype is not observed on large vessels and does not induce any major defect.

In conclusion, this study demonstrates the important and original role of PN-1 in the regulation of angiogenesis in vivo, associated with MK and, possibly, the Smad signalling pathway. It points to the strong anti-angiogenic potential of PN-1, and thus it would be of interest to study its implication in pathological mechanisms associated with angiogenesis, such as in retinal neovascular diseases.

Acknowledgments The authors thank Dr. Mary Osborne-Pellegrin for critical reading of the manuscript. This work was supported by the Institut National de la Santé et de la Recherche Médicale, University Paris 7 Denis Diderot and HemoFlu ANR-13-BSV3-0011. Sonia Selbonne and Deborah Francois were recipients of fellowships from the Fondation pour la Recherche Médicale (FRM).

References

1. O'Reilly MS, Pirie-Shepherd S, Lane WS, Folkman J (1999) Antiangiogenic activity of the cleaved conformation of the serpin antithrombin. Science 285(5435):1926–1928
2. Dawson DW, Volpert OV, Gillis P, Crawford SE, Xu H, Benedict W, Bouck NP (1999) Pigment epithelium-derived factor: a potent inhibitor of angiogenesis. Science 285(5425):245–248
3. Devy L, Blacher S, Grignet-Debrus C, Bajou K, Masson V, Gerard RD, Gils A, Carmeliet G, Carmeliet P, Declerck PJ, Noel A, Foidart JM (2002) The pro- or antiangiogenic effect of plasminogen activator inhibitor 1 is dose dependent. FASEB J 16(2):147–154
4. Becerra SP, Notario V (2013) The effects of PEDF on cancer biology: mechanisms of action and therapeutic potential. Nat Rev Cancer 13(4):258–271
5. Selbonne S, Azibani F, Iatmanen S, Boulaftali Y, Richard B, Jandrot-Perrus M, Bouton MC, Arocas V (2012) In vitro and in vivo antiangiogenic properties of the serpin protease nexin-1. Mol Cell Biol 32(8):1496–1505
6. Scott RW, Bergman BL, Bajpai A, Hersh RT, Rodriguez H, Jones BN, Barreda C, Watts S, Baker JB (1985) Protease nexin. Properties and a modified purification procedure. J Biol Chem 260(11):7029–7034
7. Evans DL, McGrogan M, Scott RW, Carrell RW (1991) Protease specificity and heparin binding and activation of recombinant protease nexin I. J Biol Chem 266(33):22307–22312
8. Bouton MC, Boulaftali Y, Richard B, Arocas V, Michel JB, Jandrot-Perrus M (2012) Emerging role of serpinE2/protease nexin-1 in hemostasis and vascular biology. Blood 119(11):2452–2457
9. Murer V, Spetz JF, Hengst U, Altrogge LM, de Agostini A, Monard D (2001) Male fertility defects in mice lacking the serine protease inhibitor protease nexin-1. Proc Natl Acad Sci USA 98(6):3029–3033
10. Lino MM, Atanasoski S, Kvajo M, Fayard B, Moreno E, Brenner HR, Suter U, Monard D (2007) Mice lacking protease nexin-1 show delayed structural and functional recovery after sciatic nerve crush. J Neurosci 27(14):3677–3685
11. Boulaftali Y, Adam F, Venisse L, Ollivier V, Richard B, Taieb S, Monard D, Favier R, Alessi MC, Bryckaert M, Arocas V, Jandrot-Perrus M, Bouton MC (2010) Anticoagulant and antithrombotic properties of platelet protease nexin-1. Blood 115(1):97–106
12. Fruttiger M (2002) Development of the mouse retinal vasculature: angiogenesis versus vasculogenesis. Invest Ophthalmol Vis Sci 43(2):522–527
13. Fruttiger M (2007) Development of the retinal vasculature. Angiogenesis 10(2):77–88
14. Luthi A, Van der Putten H, Botteri FM, Mansuy IM, Meins M, Frey U, Sansig G, Portet C, Schmutz M, Schroder M, Nitsch C, Laurent JP, Monard D (1997) Endogenous serine protease inhibitor modulates epileptic activity and hippocampal long-term potentiation. J Neurosci 17(12):4688–4699
15. Kvajo M, Albrecht H, Meins M, Hengst U, Troncoso E, Lefort S, Kiss JZ, Petersen CC, Monard D (2004) Regulation of brain proteolytic activity is necessary for the in vivo function of NMDA receptors. J Neurosci 24(43):9734–9743
16. Gerhardt H, Golding M, Fruttiger M, Ruhrberg C, Lundkvist A, Abramsson A, Jeltsch M, Mitchell C, Alitalo K, Shima D, Betsholtz C (2003) VEGF guides angiogenic sprouting utilizing endothelial tip cell filopodia. J Cell Biol 161(6):1163–1177
17. Claxton S, Fruttiger M (2005) Oxygen modifies artery differentiation and network morphogenesis in the retinal vasculature. Dev Dyn 233(3):822–828
18. Boulaftali Y, Francois D, Venisse L, Jandrot-Perrus M, Arocas V, Bouton MC (2013) Endothelial protease nexin-1 is a novel regulator of A disintegrin and metalloproteinase 17 maturation and endothelial protein C receptor shedding via furin inhibition. Arterioscler Thromb Vasc Biol 33(7):1647–1654
19. Bouton MC, Venisse L, Richard B, Pouzet C, Arocas V, Jandrot-Perrus M (2007) Protease nexin-1 interacts with thrombomodulin and modulates its anticoagulant effect. Circ Res 100(8):1174–1181
20. Chen LM, Zhang X, Chai KX (2004) Regulation of prostasin expression and function in the prostate. Prostate 59(1):1–12
21. Richard B, Arocas V, Guillin MC, Michel JB, Jandrot-Perrus M, Bouton MC (2004) Protease nexin-1: a cellular serpin down-regulated by thrombin in rat aortic smooth muscle cells. J Cell Physiol 201(1):138–145
22. Feeney SA, Simpson DA, Gardiner TA, Boyle C, Jamison P, Stitt AW (2003) Role of vascular endothelial growth factor and placental growth factors during retinal vascular development and hyaloid regression. Invest Ophthalmol Vis Sci 44(2):839–847
23. Baker JB, Gronke RS (1986) Protease nexins and cellular regulation. Semin Thromb Hemost 12(3):216–220
24. Bouton MC, Richard B, Rossignol P, Philippe M, Guillin MC, Michel JB, Jandrot-Perrus M (2003) The serpin protease-nexin 1

is present in rat aortic smooth muscle cells and is upregulated in L-NAME hypertensive rats. Arterioscler Thromb Vasc Biol 23(1):142–147
25. Choi BH, Suzuki M, Kim T, Wagner SL, Cunningham DD (1990) Protease nexin-1. Localization in the human brain suggests a protective role against extravasated serine proteases. Am J Pathol 137(4):741–747
26. Gravanis I, Tsirka SE (2005) Tissue plasminogen activator and glial function. Glia 49(2):177–183
27. Kim JA, Tran ND, Li Z, Yang F, Zhou W, Fisher MJ (2006) Brain endothelial hemostasis regulation by pericytes. J Cereb Blood Flow Metab 26(2):209–217
28. Dorrell MI, Aguilar E, Weber C, Friedlander M (2004) Global gene expression analysis of the developing postnatal mouse retina. Invest Ophthalmol Vis Sci 45(3):1009–1019
29. Dorrell MI, Friedlander M (2006) Mechanisms of endothelial cell guidance and vascular patterning in the developing mouse retina. Prog Retin Eye Res 25(3):277–295
30. Uemura A, Kusuhara S, Katsuta H, Nishikawa S (2006) Angiogenesis in the mouse retina: a model system for experimental manipulation. Exp Cell Res 312(5):676–683
31. Sommer J, Gloor SM, Rovelli GF, Hofsteenge J, Nick H, Meier R, Monard D (1987) cDNA sequence coding for a rat glia-derived nexin and its homology to members of the serpin superfamily. Biochemistry 26(20):6407–6410
32. Simonavicius N, Ashenden M, van Weverwijk A, Lax S, Huso DL, Buckley CD, Huijbers IJ, Yarwood H, Isacke CM (2012) Pericytes promote selective vessel regression to regulate vascular patterning. Blood 120(7):1516–1527
33. Balsara RD, Ploplis VA (2008) Plasminogen activator inhibitor-1: the double-edged sword in apoptosis. Thromb Haemost 100(6):1029–1036
34. Basu A, Menicucci G, Maestas J, Das A, McGuire P (2009) Plasminogen activator inhibitor-1 (PAI-1) facilitates retinal angiogenesis in a model of oxygen-induced retinopathy. Invest Ophthalmol Vis Sci 50(10):4974–4981
35. Huang Q, Wang S, Sorenson CM, Sheibani N (2008) PEDF-deficient mice exhibit an enhanced rate of retinal vascular expansion and are more sensitive to hyperoxia-mediated vessel obliteration. Exp Eye Res 87(3):226–241
36. Ota T, Ota K, Jono H, Fujimori H, Ueda M, Shinriki S, Sueyoshi T, Shinohara M, Ando Y (2010) Midkine expression in malignant salivary gland tumors and its role in tumor angiogenesis. Oral Oncol 46(9):657–661
37. Weckbach LT, Groesser L, Borgolte J, Pagel JI, Pogoda F, Schymeinsky J, Muller-Hocker J, Shakibaei M, Muramatsu T, Deindl E, Walzog B (2012) Midkine acts as proangiogenic cytokine in hypoxia-induced angiogenesis. Am J Physiol Heart Circ Physiol 303(4):H429–H438
38. Yang X, Castilla LH, Xu X, Li C, Gotay J, Weinstein M, Liu PP, Deng CX (1999) Angiogenesis defects and mesenchymal apoptosis in mice lacking SMAD5. Development 126(8):1571–1580